DMC – (R)evolution on Geometric Accuracy

CHRISTOPH DÖRSTEL, Aalen

ABSTRACT

With the introduction of digital cameras questions about various aspects of the performance of the "new digital measurement device" have started and last since then. Several investigations performed by camera users and customers as well as by some manufacturers and scientific institutes have proven the outstanding quality of digital metric cameras. However, some reports revealed systematic error pattern in the images which can be determined by self calibration parameters during bundle block adjustment. Various approaches can compensate those effects in the digital images. Intergraph with the history of the Carl Zeiss and Z/I Imaging photogrammetry business wants to deliver outstanding system performance and thus strives to research the real source for the need of additional corrections.
This paper introduces major investigation results, describes the problem and discusses applicable solutions. The main part starts with a self assessment of the Z/I Imaging calibration procedure and the DMC Post Processing System. It focusses next on a possible error budget model which leads to the approach of modeling a correction grid based on collocation technique. Finally the first results achieved with that technique are presented. The paper finishes with an outlook to the next development steps and tests at Intergraph.

1. INTRODUCTION

The DMC Digital Mapping Camera of Z/I Imaging was introduced in 2003 and several reports about the outstanding quality of DMC's radiometric and geometric performance has been published since then (Dörstel, 2003; Madani, 2004). These reports and presentations of the production site behavior of the DMC (accuracy: horizontal ±1/2 pixel / vertical ±4/5 pixel by 3001 Inc, 2004 – at GeoSpatial World 2004) have been considered as a proof of all the investigations done during system design (Tang, 2000) and system certification. However, first indications of anomalies were reported by Swedish Landmäteriet and later on this phenomenon was discussed at the EuroCow 2006 workshop in Barcelona (Alamús, 2006; Honkavara, 2006; Kruck, 2006).

At the beginning investigations concluded that systematic pattern in the block were influenced by atmospheric conditions, the camera itself, the control distribution or the introduction or weighting of additional GPS/IMU measurements. The introduction of self calibration parameters should be activated to compensate atmospheric conditions (R^3 - parameter) or other remaining influences. This was a recommendation for the adjustment process and it was not considered for the compilation from stereo models.

1.1. Problem description

For research and engineering purpose one vital and mandatory requirement is to have a proper description of the problem and the goal. In this particular case the problem description comes from the camera operator's point of view. When customers first reported their observations there were lots of discussions about difficulties with distribution or identification of control points or the weighting of GPS/IMU measurements as well as the influence from atmospheric conditions or earth curvature. One customer report (Alamús, 2006) found residuals of 0.5 – 3 [µm] in the virtual image space by analyzing the Block Rubi with an average ground sampling distance of 10 [cm]. These residuals in the image space translated into a maximum bending of 15-20 [cm] in z. In that research a preserving weighting was used and a 4 quadrant self calibration led to the correction grid as

depicted in figure 1. This correction grid when applied to other triangulations at the same approximate scale resulted in similar improvements.

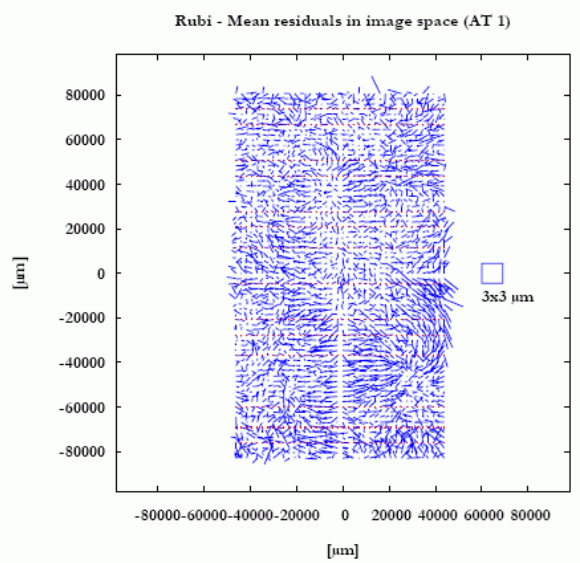

Fig. 1: Mean Residuals in image space from block Rubi (Kornus 2006)

The grid with the mean residuals showed multiple whirl structures in the individual camera segments. Similar correction shapes were found with different approaches. These structures can not be explained by regular sets of calibration parameters. They showed no appearance of influences coming from scaling or shift in the individual segments either. The investigation of a block with very high overlap in strip and cross strip directions (80% / 60% @ 6 [cm] ground resolution) has shown similar pattern.
To conclude, the goal is to research and correct a systematic distortion with a minimum estimate of 0.5 [µm] and a maximum estimate of 3 [µm]. Knowing that the random error from image measurements due to radiometric noise is about 2 [µm] this a challenging task.

2. APPLICABLE SOLUTIONS

For the practical use of DMC cameras this effect has few influences but since it is a systematic pattern we want to correct this phenomenon. In general we can distinguish between the 4 workflows, introduced in figure 2:

1. Regular workflow
2. Correction grid in Real Time Loop
3. Apply correction grid to the images
4. Improve camera calibration with correction grid

Regular workflow:
This approach (case 1.) applies to most of the projects. Excellent results can be achieved by meaningful usage of accuracies for check and control points and for the weights of GPS / IMU measurements. Applying refraction correction and self calibration parameters during bundle block adjustment process helps to achieve such good results as well. This approach is the most efficient for all projects at medium or high altitude where the vertical accuracy of the end product is not the main criterion. However some applications may require one of the following options.

Correction Grid in Real Time Loop:
Once a correction grid is computed by bundle block adjustment this can be applied in the Photogrammetric Real Time Loop while transforming measurements from the image to the object space (case 2.).

Apply correction grid to the images:
This approach requires resampling of the images a second time. In that case (3a) the second resampling degrades the image quality. To avoid quality degradation, we have introduced an interface into the DMC Post Processing software to apply the correction grid when the initial image is generated (case 3b). The correction grid can be computed from a subset of images in the project and combined with the process of a bore site calibration of the camera.

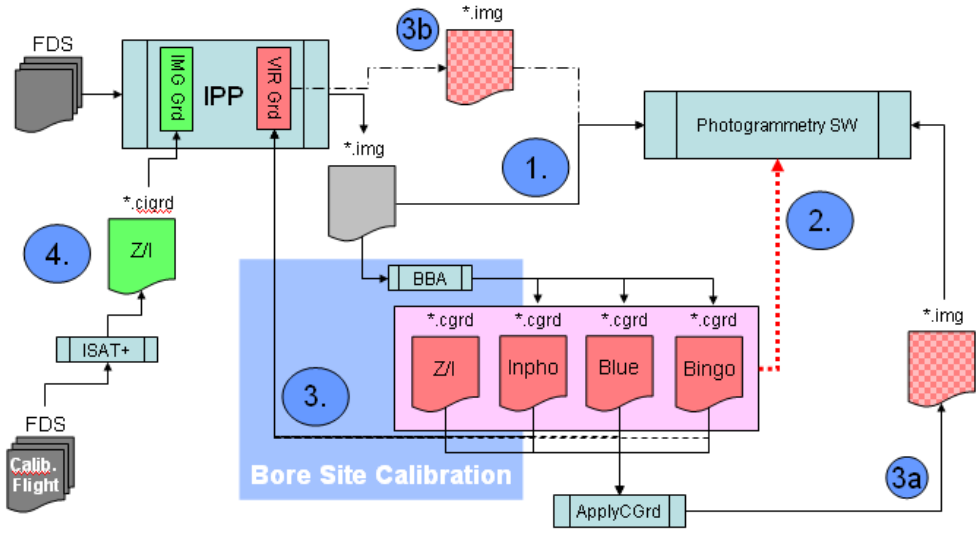

Fig. 2: Possible processing workflows for digital frame cameras – regular workflow (1), with correction grid for the Level 1 images (2) or with correction applied to images (3) or with collocation grid for improved camera calibration (4)

Improve calibration with correction grid:
This case (4.) represents the best possible solution since there is no need for additional processing within the production cycle. Because each DMC camera is delivered after a Quality Control flight (QC) performed over the Z/I test field in Elchingen, there is an established process to support this approach. The idea is to compute correction grids for the individual camera heads from high overlapping images taken over a well defined test area and to use these grids to improve the camera calibration.

3. INVESTIGATIONS

After first in-house investigations at Intergraph, where the phenomena of "systematic pattern" could not be confirmed an investigation of the "Rubi" block provided by ICC Barcelona was undertaken. From this point in time our research was accompanied by investigations of the University of Hannover, Institute for Photogrammetry and GeoInformation. Since then, lots of possibilities were discussed resulting in a systematic investigation of the complete camera calibration and the DMC Post Processing software.

3.1. Calibration and DMC Post Processing System

The aim of this research was to review the complete process of manufacturing and processing steps responsible for the final image geometry. This investigation started with a thoroughly research of the calibration device and the computational part to derive lens distortion parameters (so called Australis Parameters - AP) from the raw collimator measurements. Parts of these studies were published in 2006 by Hefele and showed that a new calibration device established at Carl Zeiss Jena has improved measurement accuracy from 1/20 to 1/25 of a pixel, resulting in a factor 2 improved σ_0 and better vertical accuracy in blocks. Further internal investigations of the post processing system researched the lens distortion correction of tie point measurements, the computation of the relative orientation of the 4 pan-chromatic camera heads and the conversion of the AP into a 1024x1024 cell-grid of 4th order polynomials (used while reading the images for rectification into the virtual image space). In short words the result of this investigation was: "It works as designed". Although this seems to be a good result it has not yet provided an explanation for the systematic pattern recognized in some of the blocks. Thus we started over with a model for a DMC error budget. We wanted to check how a maximum residual of 2 [µm] coming from the calibration process propagates into the final accuracy of check points.

3.2. Error Budget

This chapter describes how a total, non linear error in a DMC raw image propagates into the final check point measurement. The idea is to divide the total error into 3 primary sources: E1, E2 and E3 (see figure 3).

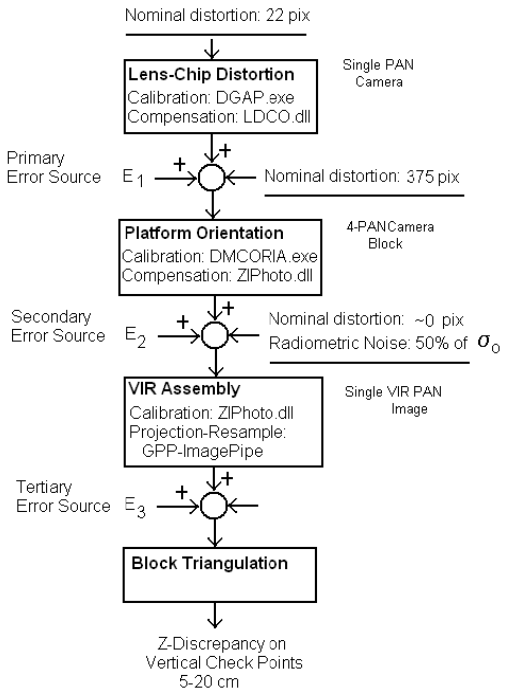

Fig. 3: Error propagation chart – from maximum nominal distortion in raw images through platform orientation, virtual image generation and block triangulation to discrepancy in check points

The lens distortion correction splits in two parts. Part one, a linear part which must be fully compensated by the platform calibration. The remaining non linear image distortion shall be called the primary error source, E1. It does not only directly propagate into VIR image, but also affects the accuracy of platform orientation as a multiplicative factor of error resulting in the secondary error source due to angular error. E1 consists of two parts (Skolnikov, 2007): A nonlinear part of systematic error after nominal 10-AP model ≈ 2[µm] (8% of total non linearity). A change in the nonlinear part due to environment is computed to ≈ 0.25[µm]. This means about 12.5% of this error is due to environmental conditions and 87.5% is due to the uncompensated constant part. This one has to be compensated first!

However, the presence of E1 distorts orientations, which results in the secondary error source, E2. E2 consists of a cumulative effect of angular and relative magnification errors:

$$E_{\Delta\omega}, E_{\Delta\varphi}, E_{\Delta\kappa}, E_{\Delta c}$$

They result mostly from systematic error in image space. As an upper limit for this error we can assume 2.5 [µm].

Virtual image assembly is a process of computing a pixel transformation map by re-projection from 4 oblique pan-chromatic cameras into a single near-nadir VIR camera and to resample the raw image data into a new composite image. All error sources in re-projection and resampling constitute the tertiary error source, E3.

This investigation leads to the conclusion that the bottleneck in VIR image distortion may be due to effects in platform orientation (E2) that easily propagates to object space. Those can be caused by insufficient compensation of non linear lens-chip distortion and thus any improvement of robustness of E1 in the platform orientation that decreases E2 should be applied. The easiest way to do this is to use the images from our test flights and to compute calibration improvement grids from a dense, well defined block.

3.3. Collocation Grid

Collocation technique in mathematics is a method for the numerical solution of differential and integral equations. The idea is to choose from finite space of candidate solutions and a number of so called collocation points, and to select that solution which satisfies the given equation at the collocation points. By using this approach all measures (collocation points) are part of the final solution.
To feature the collocation grid computation with valuable data a photogrammetric block with 80% end lap and 60% side lap shall be captured. This 80%/60% VIR block needs to be captured because it will give us a 60% by 30% overlap block for each PAN camera. The ground resolution for that investigation should be between 5 and 7 [cm]. Such a block was flown in May 2007 over the Z/I Imaging test field located in Elchingen. With that flight 846 images in 9 north-south and 12 east-west strips have been taken. The actual GSD was at 5.4 [cm] which translates to an average image scale of 1:4500. For the computation of the correction grids 33.000 observations and 37 full control points were available and the images of the individual camera heads were used. Those images can be triangulated as a regular block using ImageStation Aero Triangulation (ISAT). From the cloud of tie points a 56x32 post correction grid for each pan-chromatic camera was computed.

4. RESULTS

The grid calibration procedure produced a post-correction grid for all 4 pan-chromatic camera heads with a minimum correction of 0.3 [µm] and maximum corrections of up to 1.88 [µm]. This is from the order of magnitude what we expected to see as a correction for the individual camera heads. Comparing these results with other publications such as Kruck in 2006, he figured maximum residuals of 2.94 [µm], provides trust in that solution. Even the results from the Rubi block require corrections of a magnitude of 0.5 – 3 [µm]. Thus we can in first instance assume that the technique under discussion delivers corrections in the expected range. Looking to the shape of the corrections we saw in chapter 1.1 that the whirl structure discovered is a prominent pattern, not reproducible with standard self calibration parameters. Figure 4 shows a comparison of a correction grid modeled by Bingo and the 4 individual correction grids computed by collocation technique. The whirl structure is present in both graphics. Note, the blocks were taken with different cameras.
A more detailed analysis of the data of that test flight is currently ongoing and the final proof that the grid really resolves the block bending must still be shown.

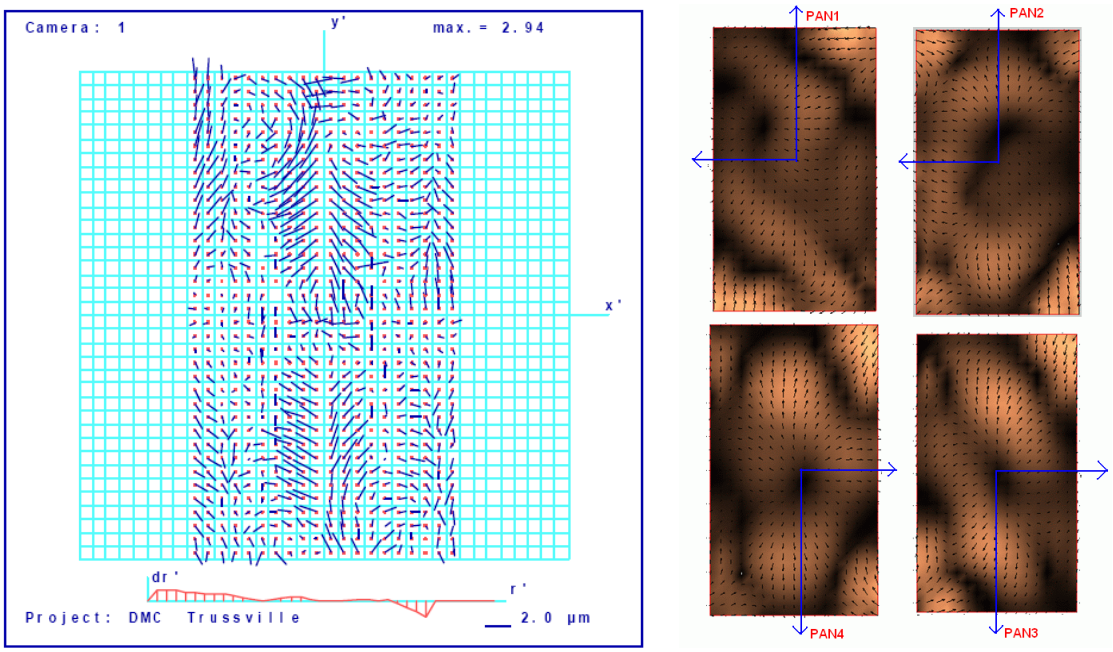

Fig. 4: visual and numerical comparision of correction grids, block Trusville (Kruck 2006) with max residual = 2.9 µm (left) and block Elchingen, max residual = 1.88 µm (right) both blocks flown with different DMC cameras.

For validation of the effectiveness of photogrammetric data refinement by post-correction, after having applied the ten AP parameters (10-AP) a QC is done. The procedure for that was as follows:

- The block is triangulated with GPS given EO StdDev of 20 [cm] and image observation StdDev of 2[um]. The triangulated XYZ objects are recorded.
- The block is triangulated with GPS given EO StdDev of 5 [cm] (Shift/Drift is active) and image observation StdDev of 6[um]. The triangulated XYZ objects are recorded.
- The estimated deformation of DTM is plotted as difference in Z between two datasets versus XY planar position.

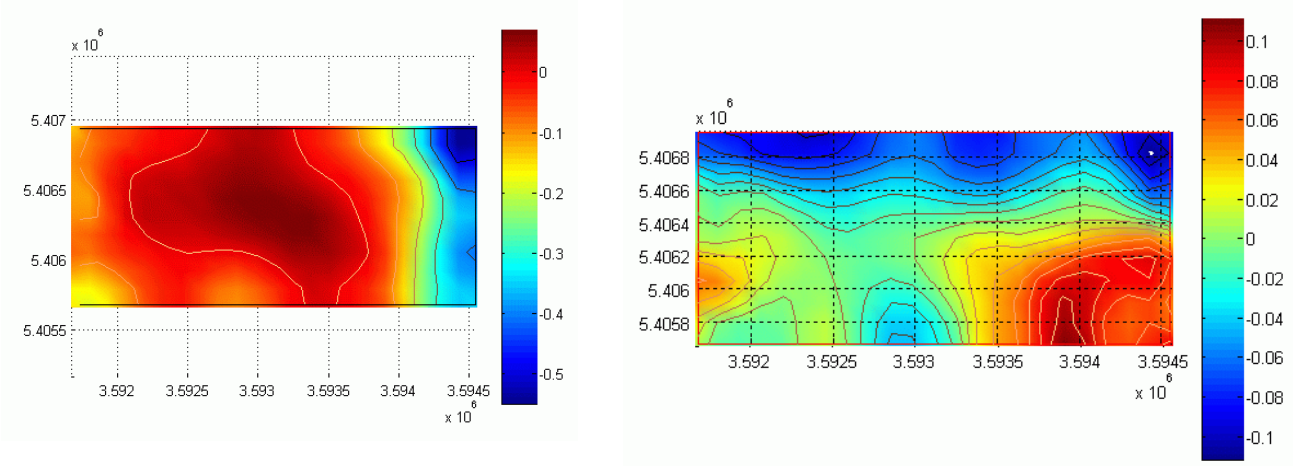

Fig. 5: DTM comparision, 10-AP correction (left) vs. Collocation grid (right)

This procedure was repeated twice: first, for a block of image observations corrected only for 10-AP by the lab calibration model and second, for a block of image observations corrected by 10-AP and post-corrected by the correction grid. This computation was done for one camera head. Figure 5

shows the results for camera head 3 where the deformation DTM was reduced from 55[cm] to 11[cm].

5. CONCLUSIONS AND OUTLOOK

In case the regular workflow for digital photogrammetry is no applied and images shall be corrected for any systematic pattern this paper introduced several possibilities. One possibility offered to the users of the DMC Post Processing software is to apply correction grids right during generation of the virtual images. This enhancement of the software guarantees best possible image quality. As a second possibility the computation of collocation grids for individual camera heads was suggested. This technique requires very well defined blocks with high overlaps. For the DMC camera this is an challenging task since the maximum residuals expected are in the order of the random error from image measurements due to radiometric noise which is about 2 [µm]. However the collocation technique introduced was capable to produce correction grids to compensate for such pattern.
Since this investigation is not completed yet the final results are still pending. The next steps to proof the correctness of the approach is to implement the collocation grid for individual camera heads into the post processing software and then to re-compute the images. The final triangulation should then confirm the proper correction of the pattern under discussion.

6. ACKNOWLEDEGEMENTS

First of all, let me give my thanks to Dr. Jakobsen from the University of Hannover and to my colleagues Dr. Ilya Shkolnikov, for his thorough investigations and Juergen Hefele and Dr. Mostafa Madani for their contribution to that paper and excellent work during our research for that topic. Special thanks of course go to our customers who provided test data sets to us and continue to help with their investigations and observations.

7. REFERENCES

Alamús, R., Kornus, W., Talaya, J. (2006): Studies on DMC Geometry. ISPRS Journal of Photogrammetry & Remote Sensing, Vol. 60, pp. 375-386.

Dörstel, C. (2003): DMC - Practical experiences and Photogrammetric System Performance, in: Fritsch D. (Ed.), Photogrammetric Week 2003, Wichmann, Heidelberg, pp. 59-65.

Hefele, J. (2006): Calibration experience with DMC. In: EuroCow 2006 Proceedings Barcelona.

Honkavaara, E., et. al. (2006): Complete Photogrammetric System calibration and Evaluation in the Sjökulla test field – Case Study with the DMC. In: Euro Cow 2006 Proceedings Barcelona.

Kruck, E. (2006): Simultaneous Calibration of Digital Aerial Survey Cameras. In: Euro Cow 2006 Proceedings Barcelona.

Madani, M., Dörstel, C., Heipke, C., Jacobsen, K. (2004): DMC practical experience and accuracy assessment. In: ISPRS Proceedings 2004 Istanbul.

Shkolnikov, I. (2007): DMC Error Budget Analysis, Technical Note, Z/I Imaging internal confidential paper.

Tang, L., Dörstel, C., Jacobsen, K., Heipke, C., Hinz, A. (2000): Geometric accuracy potential of the Digital Modular Camera, International Archives of Photogrammetry and Remote Sensing, Vol. XXXIII, Part B4/3, pp. 1051-1057.